

Transition from band insulator to Mott insulator and formation of local moment in half-filled ionic $SU(N)$ Hubbard model

Shan-Yue Wang,¹ Da Wang,^{1,2} and Qiang-Hua Wang^{1,2}

¹*National Laboratory of Solid State Microstructures and School of Physics, Nanjing University, Nanjing, 210093, China*

²*Collaborative Innovation Center of Advanced Microstructures, Nanjing University, Nanjing 210093, China*

We investigate the local moment formation in the half-filled $SU(N)$ Hubbard model under a staggered ionic potential. As the Hubbard U increases, the charge fluctuations are suppressed and eventually frozen when U is above a critical value U_c , marking the development of well-defined local moment with integer m fermions on the A-sublattice and $(N - m)$ fermions on the B-sublattice, respectively. We obtain an analytical solution for U_c for the paramagnetic ground state within the variational Gutzwiller approximation and renormalized mean field theory. For large N , U_c is found to depend on N linearly with fixed m/N , but sublinearly with fixed m . The local moment formation is accompanied by a peculiar phase transition from the band insulator to the Mott insulator, where the ionic potential and quasiparticle weight are renormalized to zero simultaneously. Inside the Mott phase, the low energy physics is described by the $SU(N)$ Heisenberg model with conjugate representations, which is widely studied in the literature.

I. INTRODUCTION

Quantum spin models are a class of physical models describing “spins” or “local moments” which originate from strong correlations between fermions (e.g. electrons or cold atoms) such that the “charge” (fermion number) degrees of freedom are frozen [1]. For instance, the Heisenberg model is a low energy description of the Hubbard model only when the Hubbard U is large enough to drive the system into the Mott insulating phase [2, 3]. In the literature, the $SU(2)$ Heisenberg model has been generalized to the $SU(N)$ case [4] with the spin operators satisfying the $SU(N)$ algebra. The $SU(N)$ Heisenberg models provide a vast area to explore many new phenomena [5–30]. Among different $SU(N)$ representations for the local spins, a conjugate representation with m fermions on A-sublattice and $(N - m)$ fermions on B-sublattice [4] is mostly studied. It may support a generalized Neel order: for instance, the first m and remaining $(N - m)$ flavors are occupied on the two sublattices, respectively. Hence, the $SU(N)$ symmetry is broken into $SU(m) \times SU(N - m)$. The gapless fluctuations above this Neel order fall into the Grassmannian manifold $\text{Gr}(N, m) = U(N)/[U(m) \times U(N - m)]$ [31–34], which is reduced to the N -component Ginzburg-Landau theory [35] or equivalently the famous CP^{N-1} model in the special case of $m = 1$.

One early motivation for doing the $SU(N)$ generalization of Heisenberg model is to perform $1/N$ expansion around the saddle point at $N = \infty$, providing a controllable way to reach the $SU(2)$ model [36]. However, physically speaking, the $SU(N)$ spin models should derive from the $SU(N)$ Hubbard model in the limit that charge fluctuations are completely frozen. The $SU(N)$ Hubbard model is widely studied, [37–50], and is now within experimental reach, thanks to the fast technical development, mostly in the field of cold atoms [51–64]. This brings the large- N model to life, but not just a gedanken model, and opens up a new field in the study of the finite but

large N versions of such models, in the search for novel quantum spin states.

However, it is important to ask under what condition is the system aptly described by the quantum spin model for which the local moments have to be well established. In our previous work, we have proposed to add a staggered ionic potential to the $SU(N)$ Hubbard model [65]. In this work, we will examine the specific conditions for the Hubbard U and ionic potential V under which the local moments can exist, with immediate relevance to experimental realization. We develop and apply an $SU(N)$ -symmetric renormalized mean field theory (RMFT) based on the variational approach of the Gutzwiller projection approximation [2, 66–71]. The RMFT developed here may be applied or extended straightforwardly for general models with a large number of fermion flavors subject to any internal symmetry. For the ionic $SU(N)$ Hubbard model, we find the local moments, with quantized integer m fermions on the A-sublattice and $(N - m)$ fermions on the B-sublattice, are well established when U is above a critical value U_c , which depends on N , m , and the ionic potential V . For large N , U_c is found to depend on N linearly with fixed m/N , but sublinearly with fixed m . In addition, the local moment formation is accompanied by a peculiar transition from the band insulator to the Mott insulator [72, 73], at which the ionic potential and quasiparticle weight are renormalized to zero simultaneously. Finally, we show that the low energy physics of local moments is described by the widely studied $SU(N)$ quantum spin model inside the Mott insulating phase. Our results shed light on the realization of such models in, e.g., cold atoms.

II. SU(N) HUBBARD MODEL IN AN IONIC POTENTIAL

The ionic SU(N) Hubbard model we consider is described by the Hamiltonian $H = H_t + H_U$, with

$$H_t = -t \sum_{\langle ij \rangle, a} [c_a^\dagger(i) c_a(j) + \text{H.c.}], \quad (1)$$

and

$$H_U = \frac{U}{2} \sum_i \left[\hat{n}(i) - \frac{N}{2} \right]^2 + V \sum_i (-1)^i \hat{n}(i), \quad (2)$$

where i labels the lattice site, $\langle ij \rangle$ denotes a nearest-neighbor bond, $a = 1, 2, \dots, N$ labels the flavor of the fermions, $\hat{n}(i) = \sum_a \hat{n}_a(i) = \sum_a c_a^\dagger(i) c_a(i)$ is the local density operator, U denotes the Hubbard interaction, and V is the staggered ionic potential. The model is clearly SU(N)-symmetric in the internal flavor space. In real space, it breaks the translational symmetry, since A- and B-sublattices are distinct. However, a particle-hole transformation $c_{ia} \rightarrow (-1)^i c_{ia}^\dagger$ interchanges these sublattices, so the system is invariant under A-B sublattice transformation combined with the particle-hole transformation. As a result, the charge density is exactly staggered and the system is at half filling on average. Such a symmetry can be used to reduce the variational parameters, as can be seen in later discussions.

The H_U -term can be rewritten as

$$H_U = \frac{U}{2} \sum_i [\hat{n}(i) - n_0(i)]^2, \quad (3)$$

where $n_0(i) = \frac{N}{2} - (-1)^i \frac{V}{U}$ may be understood as the local ground charge tunable continuously by the staggered gate voltage V . We ask whether $\hat{n}(i)$ can be quantized to integers m ($0 < m < N$) on the A-sublattice and $(N-m)$ on the B-sublattice, i.e., forming local moments, called m -tuple moments, for large enough U . The concept of local moment is a natural generalization of the SU(2) case for which only one kind of local moment with $m = 1$ is possible. Here, however, the states with different m -tuple moments should belong to different Mott insulating states. On the other hand, in the limit of $U = 0$, a nonzero V always yields a band insulator. For large enough U , the system is expected to enter different Mott insulating states labeled by m . Whether these m -tuple moments exist and how to describe these band-to-Mott insulator transitions are the main concerns of the present work. To answer these questions clearly, and for simplicity, we shall focus on the paramagnetic case in the following.

III. SU(N)-SYMMETRIC GUTZWILLER PROJECTION APPROXIMATION AND RMFT

Local moment formation is beyond any Hartree-Fock mean field description. We employ the standard

Gutzwiller projection approximation to treat the correlation effect. The SU(2) version of such a theory has been applied widely [2, 67, 68, 70, 71], and will be extended here to the SU(N)-symmetric case in which all the N -flavors are equivalent. For sufficient generality, we present the theory for an arbitrary case of the applied potential in this section, and will specify the ionic potential in the next section.

Specifically, we consider a variational theory with the following trial wave function,

$$|\psi\rangle = \hat{\mathcal{P}}|\psi_0\rangle, \quad (4)$$

where $|\psi_0\rangle$ is the ground state of a free variational Hamiltonian to be specified, and $\hat{\mathcal{P}}$ is the Gutzwiller projection operator in the grand canonical ensemble

$$\hat{\mathcal{P}} = \prod_i \hat{\mathcal{P}}_i, \quad \hat{\mathcal{P}}_i = \sum_{k=0}^N \eta_k(i) y_i^k \hat{Q}_k(i), \quad (5)$$

where $\hat{Q}_k(i)$ is the projection operator for the k -tuple state (with k -fermions),

$$\hat{Q}_k(i) = \sum_{S=\{a_\ell | \ell=1, \dots, k\}} \prod_{b \in S} \hat{n}_b(i) \prod_{b \notin S} [1 - \hat{n}_b(i)]. \quad (6)$$

Clearly, in the absence of projection, we have $\hat{\mathcal{P}}_i = \sum_k \hat{Q}_k(i) = 1$. The idea of the Gutzwiller projection is to reassign weights to the basis states, and this is how correlations (at least the local ones) can be captured. Here, the weight for the k -tuple is assumed to be

$$\eta_k(i) y_i^k = \exp(-g_i k^2 + k \ln y_i) \quad (7)$$

where g_i is the site-dependent Gutzwiller projection parameter to punish multi-fermion occupations (but can be chosen to be uniform in our case). In the spirit of density functional theory [74], the ground state energy is a unique functional of the density distribution. Therefore we have introduced a fugacity y_i to maintain the fermion density before and after projection in the grand canonical ensemble [70]. The fermion density on each site before projection is

$$N f_i = \langle \hat{n}(i) \rangle_0 = \sum_k k q_{k0}(i), \quad (8)$$

where f_i is the average occupation number per flavor, and $\langle \cdot \rangle_0$ indicates the average performed with respect to $|\psi_0\rangle$. We have defined $q_{k0}(i)$ as the average of $\hat{Q}_k(i)$ in the unprojected state,

$$q_{k0}(i) = \langle \hat{Q}_k(i) \rangle_0 = C_N^k f^k(i) [1 - f(i)]^{N-k}, \quad (9)$$

where C_N^k is the combinatorial factor. After projection, we still require

$$N f_i = \langle \hat{n}(i) \rangle = \sum_k k q_k(i), \quad (10)$$

with

$$q_k(i) = \langle \hat{Q}_k(i) \rangle = \frac{\langle \hat{\mathcal{P}} \hat{Q}_k(i) \hat{\mathcal{P}} \rangle_0}{\langle \hat{\mathcal{P}} \hat{\mathcal{P}} \rangle_0}, \quad (11)$$

where $\langle \cdot \rangle$ denotes average with respect to $|\psi\rangle$. Exact evaluation on the right hand side is difficult. To make analytical progress, we resort to the usual Gutzwiller approximation [67]: the projection operator unrelated to the target operator under average can be Wick-contracted separately. This approximation can be shown to be exact in infinite dimensions [75] for general on-site interactions [69], and turns out to work satisfactorily in finite dimensions [68, 69, 71]. Under the Gutzwiller approximation, we have

$$q_k(i) = \frac{\langle \hat{\mathcal{P}}_i \hat{Q}_k(i) \hat{\mathcal{P}}_i \rangle_0}{\langle \hat{\mathcal{P}}_i \hat{\mathcal{P}}_i \rangle_0}. \quad (12)$$

Note the projection operator \mathcal{P} is simplified to \mathcal{P}_i . After substituting $\hat{\mathcal{P}}_i$ in Eq. 5, we obtain

$$q_k(i) = \frac{\eta_k^2(i) y_i^{2k} q_{k0}(i)}{\mathcal{D}_i}, \quad \mathcal{D}_i = \sum_k \eta_k^2(i) y_i^{2k} q_{k0}(i), \quad (13)$$

where we have used $\hat{Q}_k^2(i) = \hat{Q}_k(i)$ as a property of the projection operator $\hat{Q}_k(i)$. The fugacity y_i (or $\ln y_i$ in practice) is then tuned to satisfy the density restriction Eq. 10.

After obtaining all of $q_{k0}(i)$ and $q_k(i)$, we are in a position to evaluate the variational energy in the projected state under the Gutzwiller approximation. The local charging energy is obtained most straightforwardly, given the fact that the total charge operator and the projectors $\hat{Q}_k(i)$ share the same local basis states as eigenstates,

$$E_U = \langle H_U \rangle = \frac{U}{2} \sum_i \sum_{k=0}^N [k - n_0(i)]^2 q_k(i). \quad (14)$$

The kinetic energy is slightly more difficult to evaluate. Since the fermion hopping involves two sites, we need to keep two projectors, say, $\hat{\mathcal{P}}_i$ and $\hat{\mathcal{P}}_j$ in the hopping on the $\langle ij \rangle$ bond,

$$\langle c_a^\dagger(i) c_a(j) \rangle = \frac{\langle \hat{\mathcal{P}}_i c_a^\dagger(i) \hat{\mathcal{P}}_i \hat{\mathcal{P}}_j c_a(j) \hat{\mathcal{P}}_j \rangle_0}{\langle \hat{\mathcal{P}}_i^2 \hat{\mathcal{P}}_j^2 \rangle_0}. \quad (15)$$

Since the fermion operator is self-projective, we need to remove over projections before taking the quantum average. For a given site i , we observe that

$$\begin{aligned} \hat{\mathcal{P}}_i c_a(i) \hat{\mathcal{P}}_i &= \sum_k [\eta_k(i) y_i^k \hat{Q}_k(i)] c_a(i) [\eta_{k+1}(i) y_i^{k+1} \hat{Q}_{k+1}(i)] \\ &\equiv \sum_k [\eta_k(i) \eta_{k+1}(i) y_i^{2k+1} \hat{Q}_k^{\hat{a}}(i)] c_a(i), \end{aligned} \quad (16)$$

where we have defined a partial projection operator $Q_k^{\hat{a}}(i)$ for k fermions in the local Fock space excluding flavor a ,

$$\hat{Q}_k^{\hat{a}}(i) = \sum_{S=\{a_\ell | \ell=1, \dots, k; a_\ell \neq a\}} \prod_{b \in S} \hat{n}_b(i) \prod_{b \notin S, b \neq a} [1 - \hat{n}_b(i)]. \quad (17)$$

Its average in $|\psi_0\rangle$ is evaluated to be

$$Q_k^{\hat{a}}(i) = \langle \hat{Q}_k^{\hat{a}}(i) \rangle_0 = C_{N-1}^k f_i^k (1 - f_i)^{N-1-k}, \quad (18)$$

for any flavor a in our $SU(N)$ -symmetric case. Inserting the above relations in Eq. 15, we obtain

$$\langle c_a^\dagger(i) c_a(j) \rangle = g_t(i, j) \langle c_a^\dagger(i) c_a(j) \rangle_0, \quad (19)$$

where $g_t(i, j) = z(i)z(j)$ is the renormalization of the hopping by the projection, and

$$\begin{aligned} z(i) &= \frac{\sum_k \eta_k(i) \eta_{k+1}(i) y_i^{2k+1} Q_k^{\hat{a}}(i)}{\mathcal{D}_i} \\ &= \sum_{k=0}^{N-1} Q_k^{\hat{a}}(i) \sqrt{\frac{q_k(i) q_{k+1}(i)}{q_{k0}(i) q_{k+1,0}(i)}}. \end{aligned} \quad (20)$$

In the second line we have used Eq.(13) to trade $\eta_k(i) y_i^k / \sqrt{\mathcal{D}_i}$ for $\sqrt{q_k(i) / q_{k0}(i)}$.

Combining the potential and kinetic energies, we obtain the total variational energy E in the projected state,

$$E = -t \sum_{\langle ij \rangle a} g_t(i, j) \chi_{ij0} + \frac{U}{2} \sum_i \sum_{k=0}^N [k - n_0(i)]^2 q_k(i), \quad (21)$$

where $\chi_{ij0} = \langle c_a^\dagger(i) c_a(j) + \text{H.c.} \rangle_0$ is the average of hopping operator in the unprojected state. This energy is understood as a functional of (i) the fermion density f_i which in turn depends on the trial wavefunction $|\psi_0\rangle$, and (ii) the Gutzwiller projection parameter g_i . The fugacity parameters y_i are taken as Lagrange multipliers that are eliminated by forcing the invariance of the local fermion density under the projection. The variational Gutzwiller approximation is closely related to the RMFT. Minimizing E with respect to $|\psi_0\rangle$, i.e., $\delta E / \delta \langle \psi_0 | = 0$, with fixed fermion density $N f_i$, we obtain

$$H_{\text{RMFT}} |\psi_0\rangle = \mathcal{E} |\psi_0\rangle, \quad (22)$$

where \mathcal{E} is introduced as the Lagrange multiplier enforcing normalization of the wave function, and H_{RMFT} is a free Hamiltonian yet encoded with the renormalization effect from the Gutzwiller projection,

$$H_{\text{RMFT}} = -t \sum_{\langle ij \rangle a} g_t(i, j) [c_a^\dagger(i) c_a(j) + \text{H.c.}] - \sum_i \mu_i \hat{n}(i), \quad (23)$$

where the variational local chemical potential μ_i is introduced to enforce $N f_i = \langle \hat{n}(i) \rangle_0$. It can be shown that the single-particle spectrum of H_{RMFT} is just the quasiparticle excitation spectrum beyond the correlated variational ground state, with the quasiparticle weight renormalized by g_t [70].

IV. APPLICATION TO THE IONIC $SU(N)$ HUBBARD MODEL

In this section, we apply the variational Gutzwiller approximation and RMFT developed in the previous section to the ionic $SU(N)$ Hubbard model in our interest.

A. General formalism

Due to the particle-hole and sublattice symmetries, and without involving further symmetry breaking, we only have to specify the fermion density (per flavor) f and the Gutzwiller parameter g on the A-sublattice. Correspondingly, we can replace $f \rightarrow 1 - f$, $k \rightarrow N - k$, $n_0 \rightarrow N - n_0$, etc., to obtain the relevant quantities on the B-sublattice, while g remains the same. Under these simplifications, χ_{ij0} and $g_t(i, j)$ become bond-independent, denoted as χ_0 and g_t , respectively. In particular, g_t is now given by

$$g_t = \left(\sum_k q_{k0}^{\hat{a}} \sqrt{\frac{q_k q_{k+1}}{q_{k0} q_{k+1,0}}} \right)^2. \quad (24)$$

Due to the presence of an ionic potential, we choose $\mu_i = -(-1)^i g_t \Delta_c$ in H_{RMFT} to write

$$\begin{aligned} H_{\text{RMFT}} = & -g_t t \sum_{\langle ij \rangle a} [c_a^\dagger(i) c_a(j) + \text{H.c.}] \\ & + g_t \Delta_c \sum_i (-1)^i \hat{n}(i). \end{aligned} \quad (25)$$

Under such a parametrization, g_t is a global factor renormalizing the effective bandwidth and quasiparticle excitations. The unprojected ground state $|\psi_0\rangle$, subsequently the fermion density f , and the average hopping χ_0 , only depend on Δ_c . From H_{RMFT} and after some algebra, we obtain

$$f = \frac{1}{2} \int d\varepsilon \rho(\varepsilon) \left(1 - \frac{\Delta_c}{\sqrt{\varepsilon^2 + \Delta_c^2}} \right). \quad (26)$$

$$\zeta t \chi_0 = \int d\varepsilon \rho(\varepsilon) \frac{\varepsilon^2}{\sqrt{\varepsilon^2 + \Delta_c^2}}. \quad (27)$$

Here ζ is the coordination number, and $\rho(\varepsilon)$ is the density of states. As an illustrative example, we consider the Bethe lattice, for which $\rho(\varepsilon) = (4/\pi W) \sqrt{1 - 4\varepsilon^2/W^2}$, with W the bandwidth, giving rise to

$$f = \frac{1}{2} - \frac{1}{2} \frac{\tilde{\Delta}}{\sqrt{\tilde{\Delta}^2 + 1}} {}_2F_1 \left(\frac{1}{2}, \frac{3}{2}; 2; \frac{1}{\tilde{\Delta}^2 + 1} \right), \quad (28)$$

$$\zeta t \chi_0 = \frac{W}{4} {}_2F_1 \left(\frac{1}{2}, \frac{3}{2}; 3; \frac{1}{\tilde{\Delta}^2 + 1} \right), \quad (29)$$

where $\tilde{\Delta} = 2\Delta_c/W$ and ${}_2F_1$ is the standard hypergeometric function.

In practice, for a given f , we construct q_{k0} (Eq. 9), $q_{k0}^{\hat{a}}$ (Eq. 18), and q_k (Eq. 10 by tuning y), and hence g_t (Eq. 24). Then together with χ_0 , we obtain the total variational energy (Eq. 21) per site explicitly given by

$$E = g_t E_K^0 + \frac{U}{2} \sum_k \left(k - \frac{N}{2} + \frac{V}{U} \right)^2 q_k. \quad (30)$$

where $E_K^0 = -N\zeta t \chi_0/2$. Finally, the energy E needs to be optimized with respect to (f, g) or equivalently (Δ_c, g) .

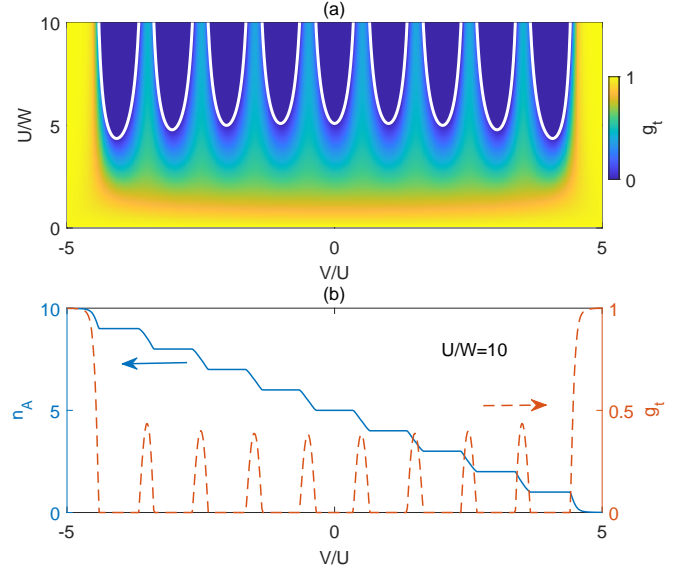


FIG. 1. Results of the ionic SU(10) Hubbard model. (a) Band renormalization factor g_t versus Hubbard U and ionic potential V . The color encodes the value of g_t . The white curves enclose Mott lobes with $g_t = 0$. (b) Fermion density n_A on the A-sublattice (solid, left scale) and g_t (dashed, right scale) versus V/U for $U/W = 10$.

B. SU(10) case

Let us take SU(10) as an example. In Fig. 1(a), we present the hopping renormalization g_t versus U and V . We find g_t is suppressed by U and drops to zero for large enough U above a critical value U_c . Interestingly, the regimes with $g_t = 0$ form different Mott lobes, enclosed by the boundaries shown as white curves (to be calculated analytically in the next section).

For $U/W = 10$, we plot the fermion density n_A on the A-sublattice (solid line, left scale) as a function of V/U in Fig. 1(b). For comparison, g_t is also plotted (dashed line, right scale). As the ionic potential V continuously varies, n_A shows a staircase behavior. Within each plateau, $n_A = m$ is quantized to the nearest integer of $n_0 = \frac{N}{2} - \frac{V}{U}$ and $g_t = 0$, where charge fluctuations are completely frozen. Between neighboring plateaus (Mott lobes), n_A changes continuously between two neighboring integers and meanwhile g_t is nonzero. In this region, the system is a band insulator with staggered charge density wave as long as $m \neq N/2$, in which there is no gapless excitation but the charge density n_A as a property of the ground state can be continuously tuned by the staggered ionic potential V . In contrast, the uniform part of the charge density (averaged over both sublattices) does not change with V , as indicated above.

In Fig. 2, we show the U -dependence of g_t , n_A , q_m and $q_{m\pm 1}$ with a fixed $V/U = 1.8$ corresponding to $m = 3$. It is seen that g_t drops continuously with U from 1 at $U = 0$ to 0 at U_c and maintains at zero for $U > U_c$. The average fermion number n_A is found to vary contin-

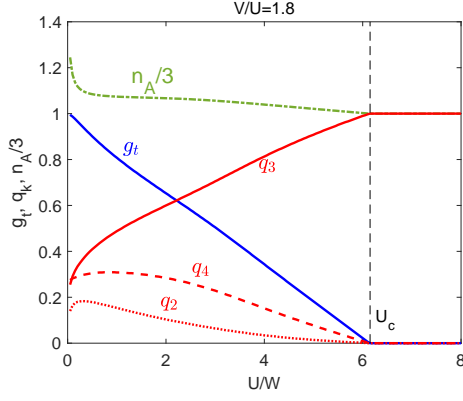


FIG. 2. Band renormalization factor g_t , average of the k -tuple projection operator q_k and fermion number n_A versus U for $V/U = 1.8$, corresponding to $m = 3$ and $\delta = 0.2$, in the case of SU(10). For clarity, only q_m and $q_{m\pm 1}$ are plotted.

uously with $U < U_c$ but quantized to m when $U \geq U_c$. The most direct way to see the local moment formation is through q_m which increases with U from the free limit value (given by Eq. 9) at $U = 0$ to 1 when $U \geq U_c$. Meanwhile, $q_{k \neq m}$ drops to zero at U_c (for clarity, only $q_{m\pm 1}$ are plotted), which of course is a natural consequence of the normalization condition $\sum_k q_k = 1$. Therefore, different m -tuple moments are well established inside these Mott insulating phases.

The phase outside of the Mott lobes are characterized by nonzero g_t , which in fact is a band insulator (except $V = 0$) caused by the ionic potential in our bipartite lattice, although there is a renormalization of the quasiparticle excitations. Therefore the phase transitions here from $g_t \neq 0$ to $g_t = 0$ are not the usual metal-insulator transitions but from the band insulator to the Mott insulator. It is an interesting question to ask whether the band gap closes to generate a metallic phase at or near the phase transition [72, 73, 76]. Our answer to this question is actually bilateral: the effective excitation gap for the quasiparticles (under projection) is given by $g_t \Delta_c$, which vanishes as the Mott limit is approached, but at the same time the quasiparticle weight also vanishes.

C. Mott transitions

We now try to obtain the critical U_c analytically for the Mott transitions. Near the Mott lobe labeled by m , we have found q_m approaches 1 and all other $q_{k \neq m}$ are small and linearly drop to zero at U_c as seen from Fig. 2. Therefore, it is reasonable to assume

$$q_k = (1 - \epsilon_- - \epsilon_+) \delta_{km} + \epsilon_- \delta_{k,m-1} + \epsilon_+ \delta_{k,m+1}, \quad (31)$$

which satisfies the normalization condition $\sum_k q_k = 1$ and gives the fermion density $Nf = \sum_k k q_k = m + (\epsilon_+ - \epsilon_-)$. The hopping renormalization Eq. 24 in this approx-

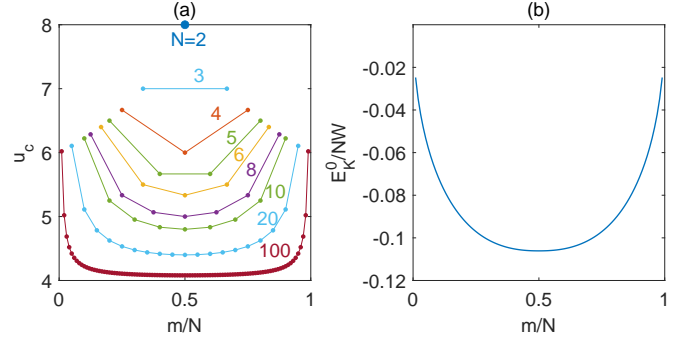


FIG. 3. (a) The universal function $u_c = U_c/|E_K^0|$ for $\delta = 0$ versus m/N for a series of N up to 100. (b) The kinetic energy per site per flavor E_K^0/N versus m/N .

imation is given by

$$g_t = \frac{1 - \epsilon_- - \epsilon_+}{q_{m0}} \left(q_{m-1,0}^{\hat{a}} \sqrt{\frac{\epsilon_-}{q_{m-1,0}}} + q_{m0}^{\hat{a}} \sqrt{\frac{\epsilon_+}{q_{m+1,0}}} \right)^2, \quad (32)$$

such that the total energy per site in the projected state becomes

$$E = -g_t |E_K^0| + \frac{U}{2}(\epsilon_- + \epsilon_+) + \frac{U}{4}(\epsilon_+ - \epsilon_-), \quad (33)$$

where we defined

$$\delta = n_0 - m = \frac{N}{2} - \frac{V}{U} - m \quad (34)$$

as the charge frustration, or the deviation of $N/2 - V/U$ away from an integer m . Requiring $\partial E / \partial \epsilon_{\pm} = 0$ in the limit of $\epsilon_{\pm} \rightarrow 0$, we obtain $U_c = u_c |E_K^0|$, with a universal function u_c independent of the details in the kinetic part of the Hamiltonian,

$$u_c = \frac{2}{1 - 2\delta} \frac{q_{m0}^{\hat{a}2}}{q_{m0} q_{m+1,0}} + \frac{2}{1 + 2\delta} \frac{q_{m-1,0}^{\hat{a}2}}{q_{m-1,0} q_{m0}}. \quad (35)$$

Using the expressions for $q_{k,0}$ (Eq. 9) and $q_{k,0}^{\hat{a}}$ (Eq. 18), it can be shown that U_c is automatically invariant under the particle-hole transformation $m \leftrightarrow N - m$ and $f \leftrightarrow 1 - f$. [We note that Eq. 35 can also be applied to the non-staggered case. The only exception is the value of χ_0 (and hence E_K^0), to be obtained in a uniform potential which in turn describes a metal.] From Eq. 35, u_c is found to depend strongly on the charge frustration δ . As $\delta \rightarrow \pm 1/2$ (maximally charge frustrated), $u_c \rightarrow \infty$, as seen in Fig. 1(a). This means the Mott transition cannot be reached in this case. For $\delta = 0$, instead, we obtain finite u_c , which we plot as a function of m/N in Fig. 3(a). In the case of $N = 2$, the Brinkman-Rice result $u_c = 8$ is recovered [2]. For larger N , u_c is reduced but always larger than 4. For a given N , u_c increases quickly as m approaches 1 or $N - 1$ but is always smaller than 8.

To proceed, we also need $|E_K^0|$ to obtain U_c . For the Bethe lattice, we plot the bare kinetic energy E_K^0 per site

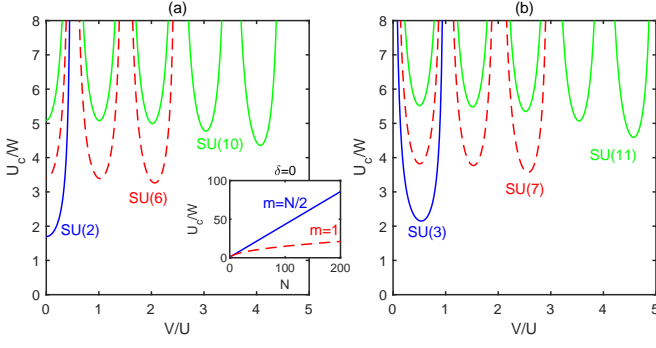


FIG. 4. (a) The critical value U_c versus V/U for $N = 2$ (solid), 6 (dashed) and 10 (dash-dotted), respectively. The Mott lobes are labeled by m . (b) U_c/W for $\delta = 0$ versus N for $m = N/2$ (solid) and $m = 1$ (dashed).

per flavor with respect to m/N in Fig. 3(b). Clearly, as m/N approaches 0 or 1, $|E_K^0|$ drops to zero. Combining u_c and $|E_K^0|$, we obtain U_c . For the cases of $N = 2, 6$ and 10 , respectively, we plot the results of U_c versus V/U in Fig. 4(a). The result of $N = 10$ is also plotted in Fig. 1(a) for comparison. Similar calculations can be performed on odd N as shown in Fig. 4(b) for $N = 3, 7$ and 11 , respectively. Note that for a fixed N (e.g., $N = 10$), U_c drops slightly as m approaches 1. This is the combined effect of the corresponding increase of u_c [see Fig. 3(a)] and decrease of $|E_K^0|$ [see Fig. 3(b)].

For the N -dependence of U_c with $\delta = 0$, we show two representative results of $m = N/2$ and $m = 1$ in the inset of Fig. 4(a). A perfect linear dependence U_c versus N for large N is seen for $m = N/2$ (solid line) since u_c approaches a constant 4 from Fig. 3(a), and $|E_K^0| \propto N$ from Fig. 3(b). We also find the scaling of $U_c \propto N$ for any fixed m/N (not shown). But for a fixed m , e.g. $m = 1$ as shown by the dashed lines in the inset of Fig. 4(a), U_c does not linearly depend on N any more. This is because m/N decreases toward zero as N increases to infinity, and thus $|E_K^0|/N$ does not maintain a fixed value but drops to zero. Therefore, the linear scaling of $U_c = u_c|E_K^0| \propto N$ breaks down to a sublinear behavior.

V. SPIN DESCRIPTION OF THE MOTT INSULATING STATES

We have found the conditions for different Mott insulating states in which different types of local moments are formed and charge degrees of freedom are frozen. The low energy effective theory inside these Mott lobes should be described by these local moments, or equivalently the $SU(N)$ “spins”.

Given the ground state with m fermions on the A-sublattice and $(N - m)$ fermions on the B-sublattice, we can perform a second order perturbation with respect to the kinetic Hamiltonian H_t , to obtain an effective Hamil-

tonian in the low energy sector,

$$H = \frac{4t^2}{(1 + \delta^2)U} \sum_{\langle ij \rangle} \sum_{ab} c_a(i)^\dagger c_b(i) c_b^\dagger(j) c_a(j), \quad (36)$$

subject to $n_i = \sum_a c_a(i)^\dagger c_a(i) = m$ on the A-sublattice and $n_i = N - m$ on the B-sublattice. This restriction suggests to define spin operators $S_{ab}(i)$ on site- i as

$$S_{ab}(i) = c_a^\dagger(i) c_b(i) - \frac{n_i}{N} \delta_{ab}, \quad (37)$$

such that the traceless condition $\text{Tr } S(i) = 0$ is satisfied. Further, it can be checked that these S_{ab} satisfy the $SU(N)$ algebra:

$$[S_{ab}, S_{cd}] = \delta_{bc} S_{ad} - \delta_{ad} S_{cb}. \quad (38)$$

Using these spin operators, the above Hamiltonian can be rewritten as the $SU(N)$ Heisenberg model

$$H = J \sum_{\langle ij \rangle ab} S_{ab}(i) S_{ba}(j), \quad (39)$$

where $J = \frac{4t^2}{(1 + \delta^2)U}$. Since $U \sim U_c$ here should be proportional to N , the above Hamiltonian has a natural large- N limit. The $SU(N)$ Heisenberg model has been widely studied in the literature, as a mathematical generalization of the $SU(2)$ Heisenberg model [4]. In this work, we have shown its relation to the ionic $SU(N)$ Hubbard model.

The above $SU(N)$ Hubbard or Heisenberg model supports an antiferromagnetic ground state with the Neel order. To represent the Neel order, we may select a specific spin axis, e.g., one of the diagonal Cartan base,

$$L_m(i) = \sum_a \ell_m^a c_a^\dagger(i) c_a(i), \quad (40)$$

with $\ell_m^a = \frac{1}{m}$ for $a \leq m$ and $-\frac{1}{N-m}$ for $a > m$. The Neel order is then described by $\langle L_m(i) \rangle \sim (-1)^i N$, with m flavors of fermions on the A-sublattice and the remaining $(N - m)$ flavors on the B-sublattice.

Note that even if the local moments L_m are ordered, the state still enjoys an internal symmetry group, $SU(m) \times SU(N - m)$, which becomes of merely gauge degrees of freedom if the charge is fully quantized. The Goldstone modes above the Neel ordered state fall into the Grassmannian manifold $\text{Gr}(N, m) = U(N)/[U(m) \times U(N - m)]$ [31]. Such fluctuations exchange the flavor content of the local moments without affecting the charge, in analogy to the spin rotation in the $SU(2)$ system.

VI. CONCLUSION

In summary, we have developed a Gutzwiller approximation and RMFT for the $SU(N)$ -symmetric fermionic

systems. Applying to the ionic Hubbard model, we find the conjugate local moments, with m fermions on the A-sublattice and $(N - m)$ fermions on the B-sublattice, are well established when the Hubbard U is above a critical value U_c . We obtained an analytical solution to U_c which depends on the bare kinematics and a universal function of m , N and the charge frustration δ . For large N , U_c is found to depend on N linearly for fixed m/N but sub-linearly with fixed m if N is fixed. The local moment formation is accompanied by a peculiar band-insulator to Mott-insulator transition, where the ionic potential and quasiparticle weight are renormalized to zero simultaneously. Inside the Mott insulating phase, the system is effectively described by the $SU(N)$ Heisenberg model which is widely studied previously in the literature. Our results shed light on the realization of such models in cold atom systems.

Finally, several remarks on the Gutzwiller projection are in order. First, it can be improved by including additional Jastrow factors [71]. Second, in one dimension, the Gutzwiller projection is inaccurate or even fails, while a long-range Jastrow factor alone (without Gutzwiller projection) turns out to be able to capture the Mott insu-

lating state correctly [77]. Third, even in infinite dimensions, the metal-Mott insulator transition is better described by the Gutzwiller projection followed by a partial Schrieffer-Wolff unitary transformation [78]. The latter two directions are intriguing and even challenge the notion of the Mott state defined by the absence of double occupancy, in the $SU(2)$ case. It would be interesting to improve our study of the slightly more complicated ionic $SU(N)$ Hubbard model along similar lines. However, we believe our results for two and higher dimensional ionic models should provide a qualitatively correct picture regarding the multiple transitions from the band insulator to Mott insulator, as well as the order of magnitude of the critical interactions.

ACKNOWLEDGMENTS

This work is supported by the National Natural Science Foundation of China (under Grant No. 11874205, No. 12274205 and No. 11574134).

-
- [1] P. W. Anderson, Localized magnetic states in metals, *Phys. Rev.* **124**, 41 (1961).
 - [2] W. F. Brinkman and T. M. Rice, Application of Gutzwiller's Variational Method to the Metal-Insulator Transition, *Phys. Rev. B* **2**, 4302 (1970).
 - [3] M. Imada, A. Fujimori, and Y. Tokura, Metal-insulator transitions, *Rev. Mod. Phys.* **70**, 1039 (1998).
 - [4] I. Affleck, Large- n limit of $SU(n)$ quantum spin chains, *Phys. Rev. Lett.* **54**, 966 (1985).
 - [5] I. Affleck and J. B. Marston, Large- n limit of the Heisenberg-Hubbard model: Implications for high- T_c superconductors, *Phys. Rev. B* **37**, 3774 (1988).
 - [6] J. B. Marston and I. Affleck, Large- n limit of the Hubbard-Heisenberg model, *Phys. Rev. B* **39**, 11538 (1989).
 - [7] D. P. Arovas and A. Auerbach, Functional integral theories of low-dimensional quantum Heisenberg models, *Phys. Rev. B* **38**, 316 (1988).
 - [8] N. Read and S. Sachdev, Valence-bond and spin-Peierls ground states of low-dimensional quantum antiferromagnets, *Phys. Rev. Lett.* **62**, 1694 (1989).
 - [9] N. Read and S. Sachdev, Some features of the phase diagram of the square lattice $SU(N)$ antiferromagnet, *Nucl. Phys. B* **316**, 609 (1989).
 - [10] N. Read and S. Sachdev, Spin-Peierls, valence-bond solid, and Neel ground states of low-dimensional quantum antiferromagnets, *Phys. Rev. B* **42**, 4568 (1990).
 - [11] K. Harada, N. Kawashima, and M. Troyer, Néel and Spin-Peierls Ground States of Two-Dimensional $SU(N)$ Quantum Antiferromagnets, *Phys. Rev. Lett.* **90**, 117203 (2003).
 - [12] F. Assaad, Phase Diagram of the Half-Filled Two-Dimensional $SU(n)$ Hubbard-Heisenberg Model: A Quantum Monte Carlo Study, *Phys. Rev. B* **71**, 075103 (2005).
 - [13] N. Kawashima and Y. Tanabe, Ground States of the $SU(N)$ Heisenberg Model, *Phys. Rev. Lett.* **98**, 057202 (2007).
 - [14] D. Arovas, Simplex solid states of $SU(N)$ quantum antiferromagnets, *Phys. Rev. B* **77**, 104404 (2008).
 - [15] C. Xu and C. Wu, Resonating plaquette phases in $su(4)$ heisenberg antiferromagnet, *Phys. Rev. B* **77**, 134449 (2008).
 - [16] C. Wu, Exotic many-body physics with large-spin fermi gases, *Physics* **3**, 92 (2010).
 - [17] K. Beach, F. Alet, M. Mambrini, and S. Capponi, $SU(N)$ heisenberg model on the square lattice: A continuous- N quantum monte carlo study, *Phys. Rev. B* **80**, 184401 (2009).
 - [18] J. Lou, A. W. Sandvik, and N. Kawashima, Antiferromagnetic to valence-bond-solid transitions in two-dimensional $SU(N)$ Heisenberg models with multispin interactions, *Phys. Rev. B* **80**, 180414 (2009).
 - [19] S. Rachel, R. Thomale, M. Fuehringer, P. Schmitteckert, and M. Greiter, Spinon confinement and the Haldane gap in $SU(n)$ spin chains, *Phys. Rev. B* **80**, 180420 (2009).
 - [20] R. K. Kaul and A. W. Sandvik, Lattice Model for the $SU(N)$ Néel to Valence-Bond Solid Quantum Phase Transition at Large N , *Phys. Rev. Lett.* **108**, 137201 (2012).
 - [21] P. Corboz, K. Penc, F. Mila, and A. M. Läuchli, Simplex solids in $SU(N)$ Heisenberg models on the kagome and checkerboard lattices, *Phys. Rev. B* **86**, 041106 (2012).
 - [22] K. Harada, T. Suzuki, T. Okubo, H. Matsuo, J. Lou, H. Watanabe, S. Todo, and N. Kawashima, Possibility of Deconfined Criticality in $SU(N)$ Heisenberg Models at Small N , *Phys. Rev. B* **88**, 220408 (2013).
 - [23] P. Nataf and F. Mila, Exact Diagonalization of Heisenberg $SU(N)$ Models,

- Phys. Rev. Lett. **113**, 127204 (2014).
- [24] J. Dufour, P. Nataf, and F. Mila, Variational Monte Carlo investigation of SU(N) Heisenberg chains, *Phys. Rev. B* **91**, 174427 (2015).
 - [25] T. Okubo, K. Harada, J. Lou, and N. Kawashima, SU(N) Heisenberg model with multi-column representations, *Phys. Rev. B* **92**, 134404 (2015).
 - [26] T. Suzuki, K. Harada, H. Matsuo, S. Todo, and N. Kawashima, Thermal phase transition of generalized Heisenberg models for SU(N) spins on square and honeycomb lattices, *Phys. Rev. B* **91**, 094414 (2015).
 - [27] P. Nataf and F. Mila, Exact diagonalization of Heisenberg SU(N) chains in the fully symmetric and antisymmetric representations, *Phys. Rev. B* **93**, 155134 (2016).
 - [28] J. D’Emidio and R. K. Kaul, First-order superfluid to valence bond solid phase transitions in easy-plane SU(N) magnets for small-n, *Phys. Rev. B* **93**, 054406 (2016).
 - [29] P. Nataf and F. Mila, Density matrix renormalization group simulations of SU(N) Heisenberg chains using standard Young tableaux: Fundamental representation and comparison with a finite-size Bethe ansatz, *Phys. Rev. B* **97**, 134420 (2018).
 - [30] F. H. Kim, F. F. Assaad, K. Penc, and F. Mila, Dimensional crossover in the SU(4) Heisenberg model in the six-dimensional antisymmetric self-conjugate representation revealed by quantum Monte Carlo and linear flavor-wave theory, *Phys. Rev. B* **100**, 085103 (2019).
 - [31] A. J. MacFarlane, Generalizations of σ -Models and Cp^N Models, and Instantons, *Phys. Lett. B* **82**, 239 (1979).
 - [32] S. Hikami, Non-Linear σ Model of Grassmann Manifold and Non-Abelian Gauge Field with Scalar Coupling, *Prog. Theor. Phys.* **64**, 1425 (1980).
 - [33] G. Duerksen, Dynamical Symmetry Breaking in Supersymmetric $U(N+m)/U(n)U(m)$ Chiral Models, *Phys. Rev. D* **24**, 926 (1981).
 - [34] J. Maharana, The canonical structure of generalized non-linear sigma models in constrained hamiltonian formalism, *Ann. IHP Phys. Théorique* **39**, 193 (1983).
 - [35] B. I. Halperin, T. C. Lubensky, and S.-K. Ma, First-order phase transitions in superconductors and smectic-A liquid crystals, *Phys. Rev. Lett.* **32**, 292 (1974).
 - [36] A. Auerbach, *Interacting electrons and quantum magnetism* (1994).
 - [37] J. P. Lu, Metal-insulator transitions in degenerate Hubbard models and A_xC_{60} , *Phys. Rev. B* **49**, 5687 (1994).
 - [38] C. Wu, J.-P. Hu, and S.-C. Zhang, Exact SO(5) Symmetry in the Spin-3/2 Fermionic System, *Phys. Rev. Lett.* **91**, 186402 (2003).
 - [39] C. Honerkamp and W. Hofstetter, Ultracold fermions and the su(n) hubbard model, *Phys. Rev. Lett.* **92**, 170403 (2004).
 - [40] K. Buchta, o. Legeza, E. Szirmai, and J. Solyom, Mott transition and dimerization in the one-dimensional SU(n) Hubbard model, *Phys. Rev. B* **75**, 155108 (2007).
 - [41] H.-H. Hung, Y. Wang, and C. Wu, Quantum magnetism in ultracold alkali and alkaline-earth fermion systems with symplectic symmetry, *Phys. Rev. B* **84**, 054406 (2011).
 - [42] Z. Cai, H.-H. Hung, L. Wang, D. Zheng, and C. Wu, Pomeranchuk Cooling of SU(2N) Ultracold Fermions in Optical Lattices, *Phys. Rev. Lett.* **110**, 220401 (2013).
 - [43] Z. Cai, H.-H. Hung, L. Wang, and C. Wu, Quantum magnetic properties of the SU(2N) Hubbard model in the square lattice: A quantum Monte Carlo study, *Phys. Rev. B* **88**, 125108 (2013).
 - [44] T. C. Lang, Z. Y. Meng, A. Muramatsu, S. Wessel, and F. F. Assaad, Dimerized Solids and Resonating Plaquette Order in SU(N)-Dirac Fermions, *Phys. Rev. Lett.* **111**, 066401 (2013).
 - [45] D. Wang, Y. Li, Z. Cai, Z. Zhou, Y. Wang, and C. Wu, Competing Orders in the 2D Half-Filled SU(2N) Hubbard Model through the Pinning-Field Quantum Monte Carlo Simulations, *Phys. Rev. Lett.* **112**, 156403 (2014).
 - [46] Z. Zhou, Z. Cai, C. Wu, and Y. Wang, Quantum monte carlo simulations of thermodynamic properties of SU(2N) ultracold fermions in optical lattices, *Phys. Rev. B* **90**, 235139 (2014).
 - [47] Z. Zhou, D. Wang, Z. Y. Meng, Y. Wang, and C. Wu, Mott insulating states and quantum phase transitions of correlated SU(2N) Dirac fermions, *Phys. Rev. B* **93**, 245157 (2016).
 - [48] Z. Zhou, D. Wang, C. Wu, and Y. Wang, Finite-temperature valence-bond-solid transitions and thermodynamic properties of interacting SU(2N) Dirac fermions, *Phys. Rev. B* **95**, 085128 (2017).
 - [49] Z. Zhou, C. Wu, and Y. Wang, Mott transition in the π -flux SU(4) Hubbard model on a square lattice, *Phys. Rev. B* **97**, 195122 (2018).
 - [50] D. Wang, L. Wang, and C. Wu, Slater and Mott insulating states in the SU(6) Hubbard model, *Phys. Rev. B* **100**, 115155 (2019).
 - [51] I. Bloch and W. Zwerger, Many-body physics with ultracold gases, *Rev. Mod. Phys.* **80**, 885 (2008).
 - [52] I. Bloch, J. Dalibard, and S. Nascimbène, Quantum simulations with ultracold quantum gases, *Nat. Phys.* **8**, 267 (2012).
 - [53] B. J. DeSalvo, M. Yan, P. G. Mickelson, Y. N. Martinez de Escobar, and T. C. Killian, Degenerate Fermi Gas of ^{87}Sr , *Phys. Rev. Lett.* **105**, 030402 (2010).
 - [54] S. Taie, Y. Takasu, S. Sugawa, R. Yamazaki, T. Tsujimoto, R. Murakami, and Y. Takahashi, Realization of a SU(2) \times SU(6) System of Fermions in a Cold Atomic Gas, *Phys. Rev. Lett.* **105**, 190401 (2010).
 - [55] J. S. Krauser, J. Heinze, N. Flaschner, S. Gotze, O. Jurgensen, D.-S. Luhmann, C. Becker, and K. Sengstock, Coherent multi-flavour spin dynamics in a fermionic quantum gas, *Nature Phys.* **8**, 813 (2012).
 - [56] S. Taie, R. Yamazaki, S. Sugawa, and Y. Takahashi, An SU(6) Mott insulator of an atomic Fermi gas realized by large-spin Pomeranchuk cooling, *Nature Phys.* **8**, 825 (2012).
 - [57] X. Zhang, M. Bishof, S. L. Bromley, C. V. Kraus, M. S. Safronova, P. Zoller, A. M. Rey, and J. Ye, Spectroscopic observation of SU(N)-symmetric interactions in Sr orbital magnetism, *Science* **345**, 1467 (2014).
 - [58] M. A. Cazalilla and A. M. Rey, Ultracold Fermi gases with emergent SU(N) symmetry, *Rep. Prog. Phys.* **77**, 124401 (2014).
 - [59] R. A. Hart, P. M. Duarte, T.-L. Yang, X. Liu, T. Paiva, E. Khatami, R. T. Scalettar, N. Trivedi, D. A. Huse, and R. G. Hulet, Observation of antiferromagnetic correlations in the Hubbard model with ultracold atoms, *Nature* **519**, 211 (2015).
 - [60] C. Laflamme, W. Evans, M. Dalmonte, U. Gerber, H. Mejía-Díaz, W. Bietenholz, U. J. Wiese, and P. Zoller, CP^{N-1} quantum field theories with alkaline-earth atoms in optical lattices, *Ann. Phys.* **370**, 117 (2016).

- [61] C. Hofrichter, L. Riegger, F. Scazza, M. Höfer, D. R. Fernandes, I. Bloch, and S. Fölling, Direct Probing of the Mott Crossover in the $SU(N)$ Fermi-Hubbard Model, *Phys. Rev. X* **6**, 021030 (2016).
- [62] H. Ozawa, S. Taie, Y. Takasu, and Y. Takahashi, Antiferromagnetic Spin Correlation of $SU(N)$ Fermi Gas in an Optical Superlattice, *Phys. Rev. Lett.* **121**, 225303 (2018).
- [63] L. Sonderhouse, C. Sanner, R. B. Hutson, A. Goban, T. Bilitewski, L. Yan, W. R. Milner, A. M. Rey, and J. Ye, Thermodynamics of a deeply degenerate $SU(N)$ -symmetric Fermi gas, *Nat. Phys.* **16**, 1216 (2020).
- [64] S. Taie, E. Ibarra-Garcia-Padilla, N. Nishizawa, Y. Takasu, Y. Kuno, H.-T. Wei, R. T. Scalettar, K. R. A. Hazzard, and Y. Takahashi, Observation of antiferromagnetic correlations in an ultracold $SU(N)$ Hubbard model, *Nature Physics* **18**, 1356 (2022).
- [65] S.-Y. Wang, D. Wang, and Q.-H. Wang, Critical exponents of the nonlinear sigma model on a Grassmann manifold $U(N)/U(m)U(N-m)$ by the $1/N$ -expansion, *Phys. Rev. B* **99**, 165142 (2019).
- [66] M. C. Gutzwiller, Effect of Correlation on the Ferromagnetism of Transition Metals, *Phys. Rev. Lett.* **10**, 159 (1963).
- [67] M. C. Gutzwiller, Correlation of Electrons in a Narrow s Band, *Phys. Rev.* **137**, A1726 (1965).
- [68] D. Vollhardt, Normal He3: an almost localized Fermi liquid, *Rev. Mod. Phys.* **56**, 99 (1984).
- [69] J. Bunemann, W. Weber, and F. Gebhard, Multiband Gutzwiller wave functions for general on-site interactions, *Phys. Rev. B* **57**, 6896 (1998).
- [70] Q.-H. Wang, Z. Wang, Y. Chen, and F. Zhang, Unrestricted renormalized mean field theory of strongly correlated electron systems, *Phys. Rev. B* **73**, 092507 (2006).
- [71] B. Edegger, V. N. Muthukumar, and C. Gros, Gutzwiller-RVB theory of high-temperature superconductivity: Results from renormalized mean-field theory and variational Monte Carlo calculations, *Adv. Phys.* **56**, 927 (2007).
- [72] A. Garg, H. R. Krishnamurthy, and M. Randeria, Can Correlations Drive a Band Insulator Metallic?, *Phys. Rev. Lett.* **97**, 046403 (2006).
- [73] S. S. Kancharla and E. Dagotto, Correlated Insulated Phase Suggests Bond Order between Band and Mott Insulators in Two Dimensions, *Phys. Rev. Lett.* **98**, 016402 (2007).
- [74] P. Hohenberg and W. Kohn, Inhomogeneous electron gas, *Phys. Rev.* **136**, B864 (1964).
- [75] F. Gebhard, Gutzwiller correlated wave functions in finite dimensions d : A systematic expansion in $1/d$, *Phys. Rev. B* **41**, 9452 (1990).
- [76] A. Chattopadhyay, S. Bag, H. R. Krishnamurthy, and A. Garg, Phase diagram of the half-filled ionic hubbard model in the limit of strong correlations, *Phys. Rev. B* **99**, 155127 (2019).
- [77] M. Capello, F. Becca, M. Fabrizio, S. Sorella, and E. Tosatti, Variational description of mott insulators, *Phys. Rev. Lett.* **94**, 026406 (2005).
- [78] M. M. Wysokiński and M. Fabrizio, Mott physics beyond the brinkman-rice scenario, *Phys. Rev. B* **95**, 161106 (2017).